JOURNAL OF MATERIALS SCIENCE 30 (1995) 1209–1216

Microwave characteristics of mixed phases of $BaTi_4O_9$–$BaPr_2Ti_4O_{12}$ ceramics

K. FUKUDA, R. KITOH
Inorganic Materials Research Laboratory, UBE Industries Ltd, 1978-5 Kogushi, Ube, Yamaguchi 755, Japan

I. AWAI
Department of Electrical and Electronic Engineering, Yamaguchi University, Tokiwadai, Ube, Yamaguchi 755, Japan

The microwave characteristics of the $BaTi_4O_9$–$BaPr_2Ti_4O_{12}$ system were investigated, including its microstructure and infrared reflection spectroscopy. It was found that this system is entirely composed of two phases, $BaTi_4O_9$ and $BaPr_2Ti_4O_{12}$, and it is suggested that the lattices of each phase are well matched obliquely at the interface in the sintered ceramics. The dielectric properties are compared with calculated values deduced from the mixing relations of the two components. Furthermore, the infrared reflection spectra of this system were analysed with the factorized form of the dielectric function, for the purpose of studying the applicability of the reflection analysis technique to this mixed phase system.

1. Introduction

Most microwave dielectric ceramics used in mobile communication systems and satellite broadcasting systems are composed of a single phase, which has excellent microwave characteristics e.g. $Ba(Zn_{1/3}Ta_{2/3})O_3$ [1], $Ba_2Ti_9O_{20}$ [2] and $BaSm_2Ti_5O_{14}$ [3].

In order to obtain the desired dielectric properties, the mixing technique of two low loss materials, with positive and negative dielectric temperature coefficients, has become well known. As reported by Paladino [4], zero temperature coefficient of the resonant frequency, τ_f, was achieved at an intermediate composition of $MgTi_2O_5$–TiO_2 system. This approach should have wide applicability, if the proper selection of two compounds is carried out. However, in general, it is not easy to realize a material with intermediate properties in such two components system because of the difficulty in retaining their individual properties at the sintering temperature. Therefore, as a basis for development of a dielectric material system perfectly composed of two compounds, it is necessary to investigate the system's microstructure and dielectric properties.

As one possible selection of two compounds, the TiO_2–Bi_2O_3 system, composed of two phases, TiO_2 and $Bi_2Ti_4O_{11}$ has already been investigated; the mixing relation for microwave dielectric properties, particularly, for Q values, has been examined [5]. As a result, it was found that the Q values of mixtures are determined from the volume fraction and Q value of each component; in a similar manner to the dielectric constant and temperature coefficient [4].

In this study, as another possible selection, the microstructure and microwave dielectric properties of the $BaTi_4O_9$–$BaPr_2Ti_4O_{12}$ system is examined. For the microstructure, the ceramic interface, which is considered to influence the dielectric properties on this system, is studied. Furthermore, infrared reflection analysis of this system was carried out to obtain quantitative dielectric data.

2. Experimental procedure

Ceramic samples were prepared with high purity $BaCO_3$, TiO_2 and Pr_6O_{11}. The powders were weighed to obtain a composition of $(1-x)$-$BaTi_4O_9$–x $BaPr_2Ti_4O_{12}$($x = 0$, 0.17, 0.36, 0.56, 0.77 and 1.00), ball milled, dried and calcined at 1000 °C for 2 h. Following the addition of organic binder, the mixture was pressed into pellets and sintered at 1300–1550 °C for 2 h. The dielectric characteristics of these sintered ceramics were measured using the resonant cavity method in the $TE_{01\delta}$ mode [6].

The infrared reflection spectra were obtained using a Fourier transform spectrometer, Broker IFS-113V. A glow-bar lamp was used for measurement from 50 to 4000 cm^{-1}. A polished ceramic was set in the vacuum chamber evacuated to 1.3 Pa, and the reflectivities were measured relative to the reflectance of an evaporated gold mirror. The incident angle of radiation was 11 °, and the spectra were recorded at a resolution of 1 cm^{-1}.

The reflectance data were transformed to dielectric data with the factorized form proposed by Gervais and Piriou [7], instead of the classical dispersion theory, considering that vibrational modes with

0022–2461

different energy levels should not be equally damped [8]. The frequency-dependent complex dielectric function is then written as

$$\varepsilon = \varepsilon_\infty \prod_j \frac{\Omega_{jLO}^2 - \omega^2 + i\gamma_{jLO}\times\omega}{\Omega_{jTO}^2 - \omega^2 + i\gamma_{jTO}\times\omega} \quad (1)$$

where Ω_{jTO} and γ_{jTO} are the transverse optic (TO) mode frequency and its damping constant; and Ω_{jLO} and γ_{jLO} are the longitudinal optic (LO) mode frequency and its damping constant, respectively. Equation 1 can be regarded as an extended Lyddane–Sachs–Teller (LST) relation [9, 10] in which damping terms are induced. Infrared reflection spectra R were fitted with the aid of Equation 1 together with

$$R = \left|\frac{(\varepsilon^{1/2} - 1)}{(\varepsilon^{1/2} + 1)}\right|^2 \quad (2)$$

The oscillator strength $\Delta\varepsilon_j$ [8] and the quality factor Q can then be obtained from

$$\Delta\varepsilon_j = \varepsilon_\infty\left(\frac{\Omega_{jLO}^2}{\Omega_{jTO}^2} - 1\right)\prod_{k\neq j}\frac{\Omega_{kLO}^2 - \Omega_{jTO}^2}{\Omega_{kTO}^2 - \Omega_{jTO}^2} \quad (3)$$

$$Q = 1/\tan\delta = \frac{\varepsilon'}{\varepsilon''} \quad (4)$$

The microwave dielectric loss of each TO mode is calculated by the following equation [11] under the conditions $\omega^2 \ll \Omega_{jTO}^2$

$$\tan\delta_j = \frac{\Delta\varepsilon_j(\gamma_{jTO}\times\omega)/\Omega_{jTO}^2}{\varepsilon_\infty + \sum_i \Delta\varepsilon_i} \propto \frac{\gamma_{jTO}\times\omega}{\Omega_{jTO}^2} \quad (5)$$

3. Results and discussion

3.1. Microstructure

It is well known that in the BaO–TiO_2 system numerous phases, e.g. $BaTi_3O_7$, $BaTi_4O_9$ and $Ba_2Ti_9O_{20}$ exist [12]. Furthermore, various phases are also observed in the BaO–TiO_2–rare earth oxide system [13]. Therefore, phase control is expected to be extremely difficult in such a system. However, it was found that the $(1-x)BaTi_4O_9$–$xBaPr_2Ti_4O_{12}$ system given here is composed of only two phases, $BaTi_4O_9$ and $BaPr_2Ti_4O_{12}$. In fact, no peaks are observed except for those for $BaTi_4O_9$ and $BaPr_2Ti_4O_{12}$, as shown in the X-ray diffraction (XRD) patterns, Fig. 1. The XRD patterns of pure $BaTi_4O_9$ ($x = 0$) and $BaPr_2Ti_4O_{12}$ ($x = 1.0$), measured as a standard, are almost the same as ones reported previously [14].

From scanning electron microscopy (SEM) observations of polished and thermally-etched (at 1200 °C for 10 min) cross-sections of two ceramic samples ($x = 0.36$ and 0.77 in Fig. 1, respectively), it is obvious that grains can be divided into two classes, grey parts and white parts; and these grains are in coexistence without interference, as illustrated in Fig. 2a, b, as the backscattering electron image. X-ray microanalysis (XMA) shows that grey grains (spot 1 in Fig. 2b) are composed of only $BaTi_4O_9$ (spot 2 in Fig. 2b) and the white grains are composed of only $BaPr_2Ti_4O_{12}$.

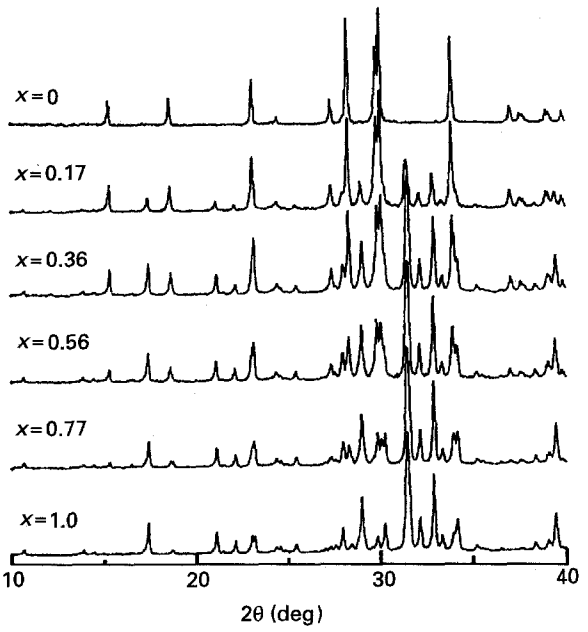

Figure 1 XRD patterns of ceramic samples in the $(1-x)BaTi_4O_9$–$xBaPr_2Ti_4O_{12}$ system.

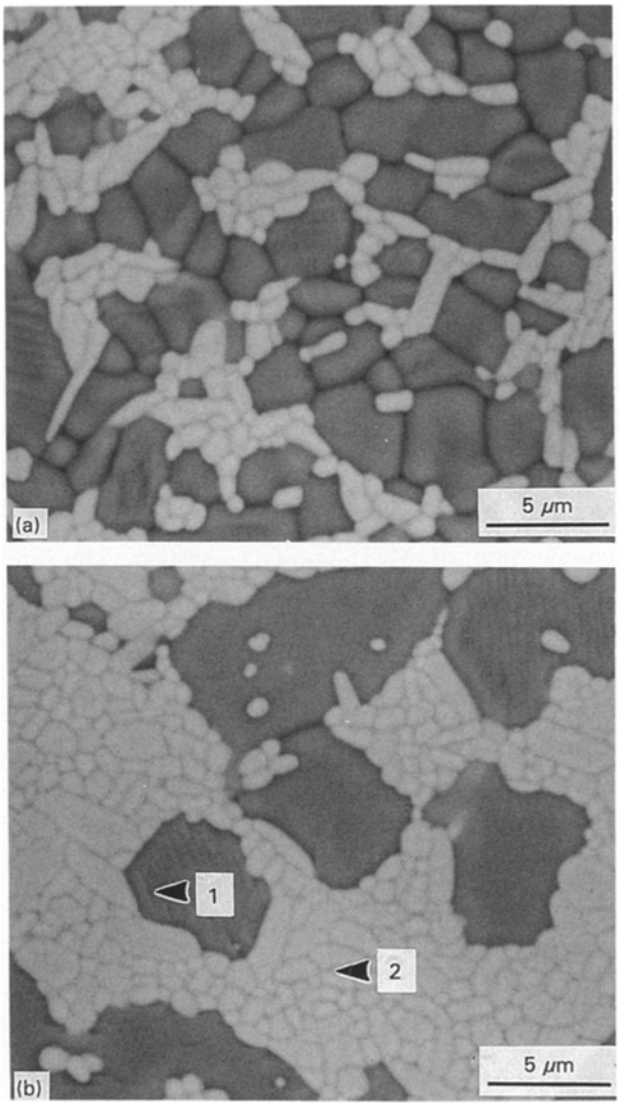

Figure 2 SEM photographs of ceramic samples in the $(1-x)$-$BaTi_4O_9$–$xBaPr_2Ti_4O_{12}$ system; backscattering electron image of (a) $x = 0.36$, and (b) $x = 0.77$.

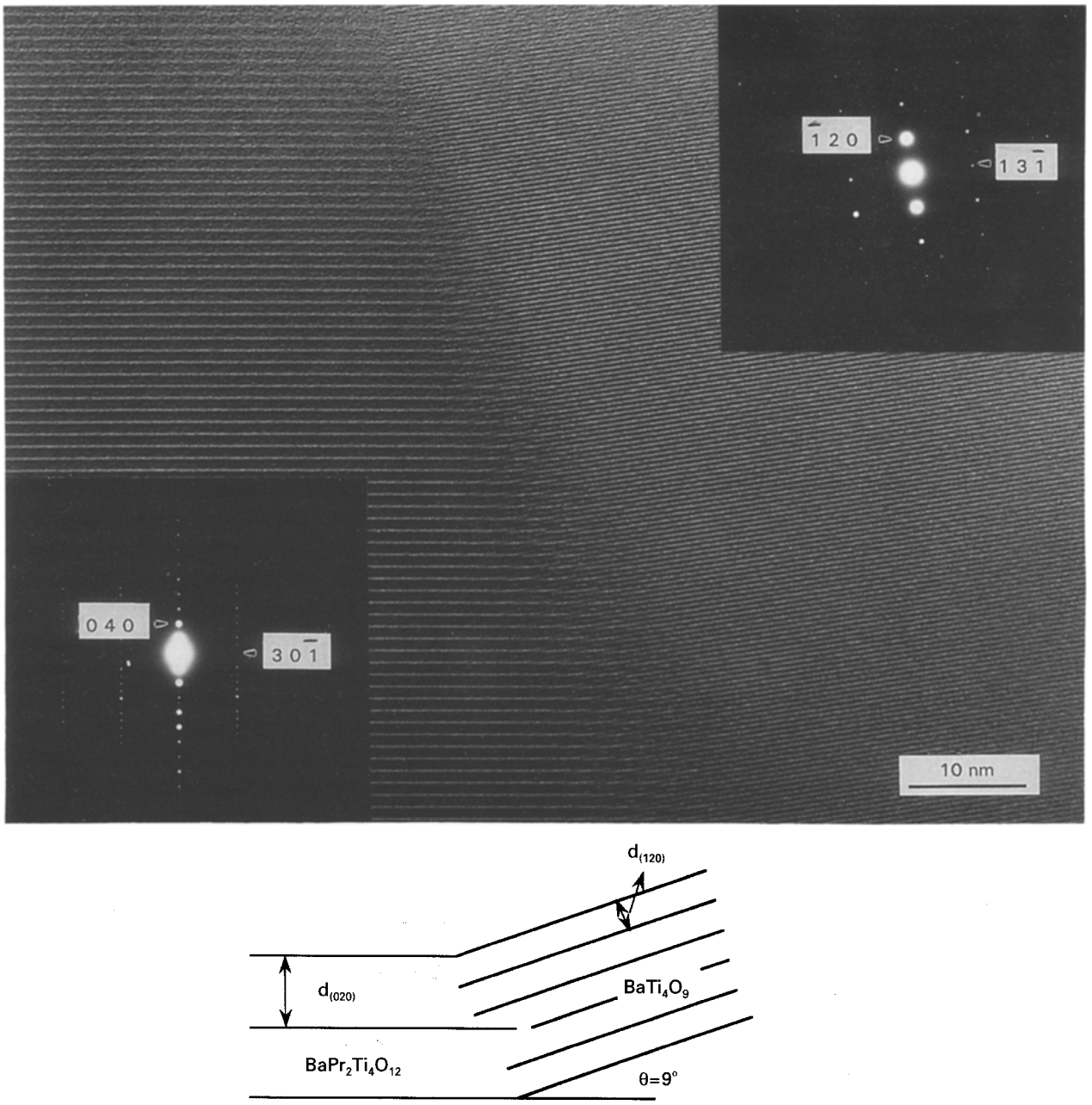

Figure 3 TEM photographs of ceramic sample ($x = 0.36$ in Fig. 1).

These results correspond well with the XRD data displayed in Fig. 1. Of particular interest is the behaviour at the interface of two phases seen by transmission electron microscopy (TEM), as shown in Fig. 3 by electron diffraction images of the ceramic sample ($x = 0.36$ in Fig. 1). In contrast with expectations that the interface of each phase consists of a disturbed array of atoms, with a thickness of a few nanometres, the lattices of each phase are well matched obliquely (about 9°); i.e. double widths of the (0 2 0) plane for $BaPr_2Ti_4O_{12}$ are nearly equivalent to the five-fold widths of the (1 2 0) plane for $BaTi_4O_9$ at the interface (this observation can also be supported by a simple calculation using each lattice parameter, $d_{(0\,2\,0)} = 1.115$ nm [15] and $d_{(1\,2\,0)} = 0.475\,74$ nm). Although it is necessary to observe various points in the ceramics for the matched interface, this fact may be related to the result that each phase can preserve its properties at the sintering temperature in this system.

3.2. Microwave properties and mixing relation

As shown in Figs 1 and 2, the system $BaTi_4O_9$–$BaPr_2Ti_4O_{12}$ ceramics is entirely composed of two phases, and in such a case it should be possible to predict the dielectric properties of the mixtures from dielectric properties of each component. The empirical models for predicting dielectric constants [4], temperature coefficients [4] and Q values [5] are expressed as follows

$$\ln \varepsilon = V_1 \ln \varepsilon_1 + V_2 \ln \varepsilon_2 \quad (6)$$

$$\tau = V_1 \tau_1 + V_2 \tau_2 \quad (7)$$

$$1/Q = V_1/Q_1 + V_2/Q_2 \quad (8)$$

where V_1 and V_2 are the volume fractions of the two components; ε_1 and ε_2 are their dielectric constants, while ε is the resultant dielectric constant of the

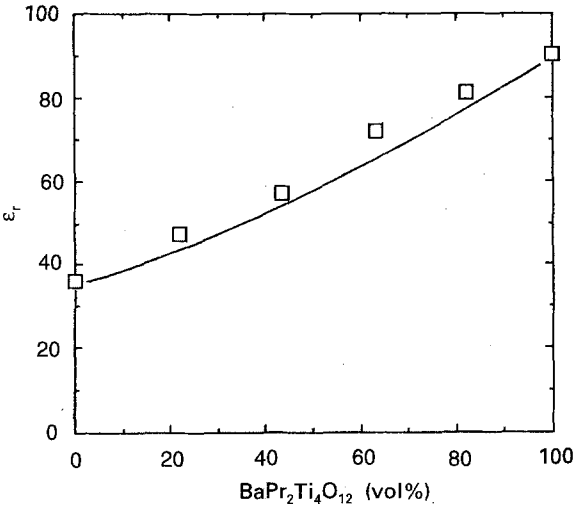

Figure 4 Room temperature dielectric constant, ε_r, versus volume fraction of $BaPr_2Ti_4O_{12}$ in the $BaTi_4O_9$–$BaPr_2Ti_4O_{12}$ system. The solid curve represents values from the mixing relation, Equation 6.

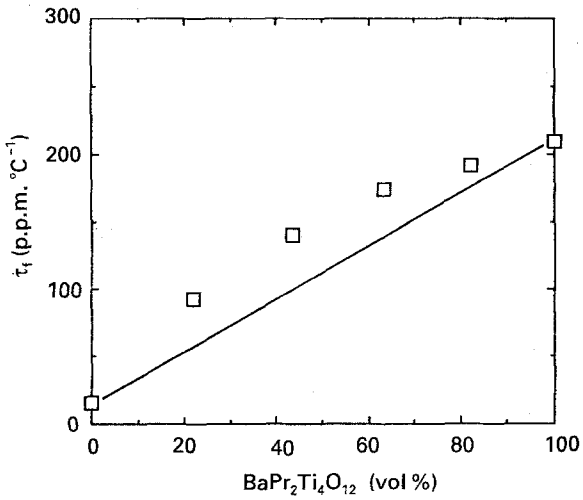

Figure 5 τ_f versus volume fraction of $BaPr_2Ti_4O_{12}$ in the $BaTi_4O_9$–$BaPr_2Ti_4O_{12}$ system. The solid line represents values from the mixing relation, Equation 7.

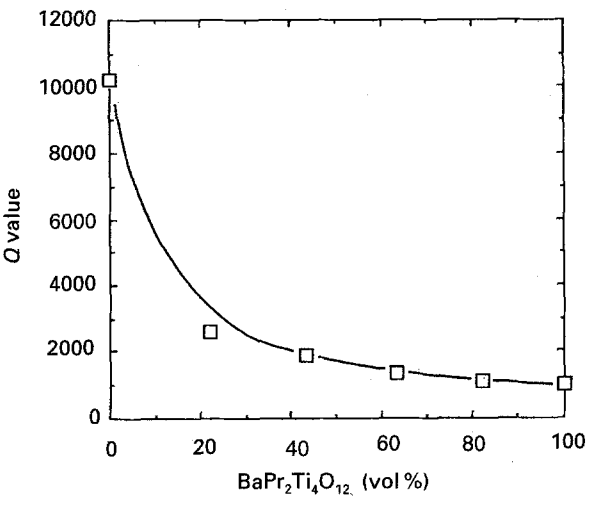

Figure 6 Q value versus volume fraction of $BaPr_2Ti_4O_{12}$ in the $BaTi_4O_9$–$BaPr_2Ti_4O_{12}$ system. The solid curve represents values from the mixing relation, Equation 8.

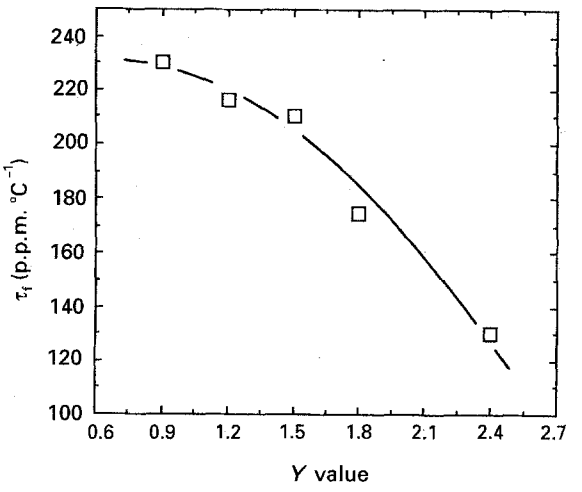

Figure 7 τ_f of $Ba_{6-y}Pr_{8+2/3y}Ti_{18}O_{54}$ ceramics.

mixture; τ_i is the temperature coefficient; and Q_1 and Q_2 are the Q values of the two components. The room temperature dielectric constants, ε_r, the temperature coefficient of resonant frequency, τ_f, and Q values are shown in Figs 4–6, respectively, compared with those obtained from the mixing relations, Equations 6–8. The volume fraction of each component is calculated on the assumption that the ceramic samples are perfectly composed of $BaTi_4O_9$ and $BaPr_2Ti_4O_{12}$. From Fig. 6 it is found that the values of the measured Q values lie on the curve calculated from Equation 8, which indicates that this equation, for representing the mixing relation for Q values, is effective for predicting that of the mixture. On the other hand, the values of dielectric constants, and particularly those of τ_f, fail to fall on the curves calculated from Equations 6 and 7. Though the origin of this result is now uncertain, it is considered that formation of the solid solution expressed by the general formula $Ba_{6-y}Pr_{8+2y/3}Ti_{18}O_{54}$ [16] is strongly concerned with this result. The phase $BaPr_2Ti_4O_{12}$ is the intermediate composition of $y = 1.5$ in this formula. Obtained was the experimental result that τ_f for $Ba_{6-y}Pr_{8+2/3y}Ti_{18}O_{54}$ ceramics rapidly increases with the decrease in y value, maintaining the same crystal structure as shown in Fig. 7. Accordingly, it is deduced that $Ba_{6-y}Pr_{8+2/3y}Ti_{18}O_{54}$ ceramics ($y < 1.5$) with higher τ_f compared to the $BaPr_2Ti_4O_{12}$ ceramic, was formed in the vicinity of $x = 0.5$ in the $(1-x)$-$BaTi_4O_9$–$xBaPr_2Ti_4O_{12}$ ceramic system. It is necessary to investigate this phenomenon in more detail.

3.3. Infrared reflection analysis

So far, the reflectance spectra of dielectric materials were usually analysed according to the classical dispersion theory or to the Kramers–Kronig relation [11, 17–19], and these results suggest that infrared reflectance spectroscopy could be used for the characterization of dielectric ceramics. This technique was applied with the factorized model described in

TABLE I Frequencies and damping parameters of three ceramics as deduced from the best fit to the reflectivity data

	$BaPr_2Ti_4O_{12}$				$0.64BaPr_2Ti_4O_{12}$–$0.36BaTi_4O_9$				$BaTi_4O_9$			
j	Ω_{jTO} (cm^{-1})	γ_{jTO} (cm^{-1})	Ω_{jLO} (cm^{-1})	γ_{jLO} (cm^{-1})	Ω_{jTO} (cm^{-1})	γ_{jTO} (cm^{-1})	Ω_{jLO} (cm^{-1})	γ_{jLO} (cm^{-1})	Ω_{jTO} (cm^{-1})	γ_{jTO} (cm^{-1})	Ω_{jLO} (cm^{-1})	γ_{jLO} (cm^{-1})
1	77.0	14.1	78.9	13.0	60.7	3.0	61.5	3.0	60.0	1.0	61.0	1.0
2	91.6	17.9	100.0	16.5	76.8	6.5	81.4	6.5	75.1	4.0	80.4	4.0
3	116.0	24.7	121.2	22.0	91.1	12.0	98.3	14.0	82.7	4.0	85.9	4.0
4	135.7	32.7	154.2	30.0	121.7	27.0	124.1	24.0	99.4	5.0	103.4	5.0
5	173.8	40.5	187.0	40.0	138.9	53.0	159.0	53.0	147.9	33.0	148.0	33.0
6	204.0	43.4	225.7	43.1	170.2	45.9	183.6	50.0	160.9	10.0	161.8	12.9
7	234.3	44.5	269.0	45.0	209.9	19.1	214.2	18.1	169.2	12.9	177.8	9.0
8	274.0	29.5	280.5	30.1	229.1	18.2	246.2	21.0	212.0	6.1	212.7	6.1
9	284.5	29.5	306.7	29.5	259.9	15.0	263.8	15.0	230.5	7.2	238.4	10.0
10	314.6	31.0	340.5	31.0	269.9	17.0	281.4	17.0	243.6	5.0	246.1	5.0
11	341.8	34.5	379.2	34.5	288.1	18.5	309.3	14.5	259.9	10.0	267.2	17.0
12	384.3	33.0	407.5	34.0	314.3	17.0	326.7	23.0	286.5	15.0	309.5	13.0
13	409.5	39.0	441.5	36.5	332.8	45.0	370.2	49.5	317.0	9.0	319.5	9.0
14	448.4	35.0	486.0	35.5	387.7	43.8	406.0	43.5	327.7	23.0	343.0	13.0
15	490.0	41.0	499.0	42.0	427.2	38.0	449.8	32.0	376.8	37.8	400.0	29.5
16	542.5	42.0	552.0	40.0	453.1	27.0	476.0	27.0	436.2	27.0	460.2	18.0
17	567.0	53.5	617.0	51.0	487.0	32.0	503.3	32.0	467.8	30.0	478.0	30.0
18	618.5	40.5	712.5	40.5	511.2	26.6	530.5	26.2	492.6	23.6	527.3	18.9
19	717.5	44.0	764.2	55.0	543.3	28.0	553.1	29.0	535.6	24.0	552.4	21.0
20	819.0	64.0	838.0	67.0	546.2	39.5	627.5	50.2	560.2	27.0	605.5	53.0
21					625.7	50.0	626.4	52.3	625.7	50.0	626.2	55.0
22					639.9	50.0	735.5	52.0	632.6	86.0	742.5	57.0
23					736.6	40.0	761.9	53.0	746.1	51.0	752.1	51.0
24					791.6	78.0	824.5	72.0	758.1	77.0	828.5	56.0
25					920.2	69.5	936.5	67.5	920.2	74.5	949.5	17.5
	$\varepsilon_\infty = 5.09$				$\varepsilon_\infty = 4.04$				$\varepsilon_\infty = 4.80$			

TABLE II Calculated $\Delta\varepsilon_j$ and $\tan\delta_j$ for each TO mode

	$BaPr_2Ti_4O_{12}$		$0.64BaPr_2Ti_4O_{12}$–$0.36BaTi_4O_9$		$BaTi_4O_9$	
j	$\Delta\varepsilon_j^a$	$\tan\delta_j^b$ ($\times 10^{-3}$)	$\Delta\varepsilon_j$	$\tan\delta_j$ ($\times 10^{-3}$)	$\Delta\varepsilon_j$	$\tan\delta_j$ ($\times 10^{-3}$)
1	8.20	0.03589	2.19	0.00529	1.76	0.0020
2	20.68	0.08117	9.87	0.03217	6.92	0.0219
3	9.62	0.03251	6.91	0.02954	0.89	0.0023
4	17.57	0.05740	2.97	0.01604	1.68	0.0038
5	9.04	0.02231	12.06	0.09797	0.05	0.0003
6	10.47	0.02009	2.56	0.01201	0.68	0.0017
7	4.49	0.00669	1.70	0.00218	2.91	0.0059
8	0.81	0.00585	4.36	0.00447	0.29	0.0001
9	1.11	0.00745	1.37	0.00090	3.14	0.0019
10	1.39	0.00803	2.14	0.00147	0.44	0.0001
11	0.17	0.00093	1.67	0.00110	1.83	0.0012
12	0.31	0.00129	0.58	0.00029	3.62	0.0029
13	0.09	0.00041	0.71	0.00086	0.23	0.0000
14	0.18	0.00058	0.61	0.00053	0.93	0.0008
15	0.02	0.00008	1.05	0.00065	1.93	0.0023
16	0.43	0.00112	0.16	0.00006	2.16	0.0013
17	0.78	0.00239	0.28	0.00011	0.39	0.0002
18	0.03	0.00006	0.21	0.00006	1.13	0.0004
19	0.02	0.00002	0.23	0.00007	0.32	0.0001
20	0.04	0.00007	0.40	0.00015	0.33	0.0001
21			0.00	0.00000	0.03	0.0000
22			0.15	0.00006	0.57	0.0005
23			0.00	0.00000	0.01	0.0000
24			0.04	0.00001	0.04	0.0000
25			0.04	0.00001	0.08	0.0000

[a] Calculated using Equation 3. [b] Calculated using Equation 5 for each TO mode at 5 GHz.

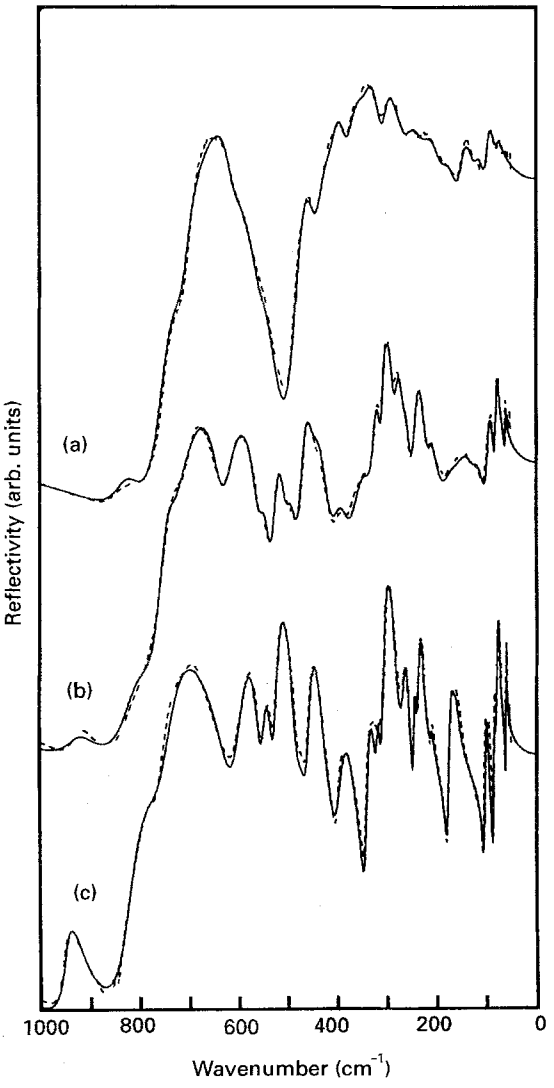

Section 2, instead of the classical dispersion theory to the material system composed of mixed phases mentioned above. Fig. 8a–c demonstrates the measured and calculated reflectance spectra of $BaPr_2Ti_4O_{12}$, $0.64BaTi_4O_9$–$0.36BaPr_2Ti_4O_{12}$, and $BaTi_4O_9$ ceramics, respectively. The solid lines show the calculated reflectivity, which are in good agreement with the observed ones (dashed lines) for the three ceramics. An attempt was also made to fit the reflectivity data with the classical dispersion theory, but the calculated reflectivities data did not fit the observed ones well; which suggests that vibrational modes with different energy levels should not be equally damped [8]. Table I shows the frequencies and damping parameters deduced from the best fit of the reflectivity data for these ceramics, and Table II summarizes $\Delta\varepsilon_j$ and $\tan\delta_j$ calculated using Equations 3 and 5. In $BaPr_2Ti_4O_{12}$ ceramics, the observed reflectance spectrum was found to be well fitted by using 20 phonons in total (Fig. 8a). It was found that six phonons ($j = 1$–6) having low resonant frequencies of 80–220 cm^{-1} had large oscillator strength ($\Delta\varepsilon_j > 8$), and thus contributed significantly to dielectric loss at microwave frequencies. In a previous work [20] where measurement of the reflectance spectrum of $BaPr_2Ti_5O_{14}$ ceramics, whose crystal structure was analogous to that of $BaPr_2Ti_4O_{12}$, 18 infrared modes were observed. The general appearance of the $BaPr_2Ti_4O_{12}$ ceramics spectrum is similar to that of $BaPr_2Ti_5O_{14}$, but the $BaPr_2Ti_5O_{14}$ peaks located at 200–400 cm^{-1} are

Figure 8 Measured (---) and calculated (——) reflectivity for (a) $BaPr_2Ti_4O_{12}$, (b) $0.64BaTi_4O_9$–$0.36BaPr_2Ti_4O_{12}$ and (c) $BaTi_4O_9$ ceramics.

sharper than those of the $BaPr_2Ti_4O_{12}$ ceramics. In $0.64BaTi_4O_9$–$0.36BaPr_2Ti_4O_{12}$ ceramics, it is found that three phonons ($j = 2, 3, 5$) have great strength ($\Delta\varepsilon_j > 6$) and resonant frequencies were shifted to relatively higher frequencies compared with those of the $BaPr_2Ti_4O_{12}$ ceramics. This observation can be seen clearly from Fig. 9, where computed ε'' as a function of frequency is shown. On the other hand, the observed reflectance spectrum of the $BaTi_4O_9$ ceramics was found to be well fitted using 25 phonons in total (Fig. 8b), and many resonances ($j = 1, 2, 4, 9, 11, 12, 15, 16, 18$), with the same degree of intensity and damping, are distributed in a wide range of lower to higher frequencies (50 to 500 cm^{-1}) as shown in Fig. 9.

The room temperature dielectric constant, ε_r and Q from Equations 1 and 4 are compared with those obtained from direct measurements at 5 GHz in Table III for three ceramics. The calculated dielectric constant agree well with the measured values, and the calculated Q values are to some extent larger than the measured ones for the $BaPr_2Ti_4O_{12}$ and $0.64BaTi_4O_9$–$0.36BaPr_2Ti_4O_{12}$ ceramics. The origin of the difference in Q values may be the result of an error in the reflectance measurements, due to factors such as scattering from porosity and scratches on the ceramic samples, as reported by Mhaisalkar *et al.* [18]. Though such problems must be solved for better estimation, it is suggested that this method of reflection analysis can be applied to such ceramic materials composed of mixed phases for investigating the dielectric properties.

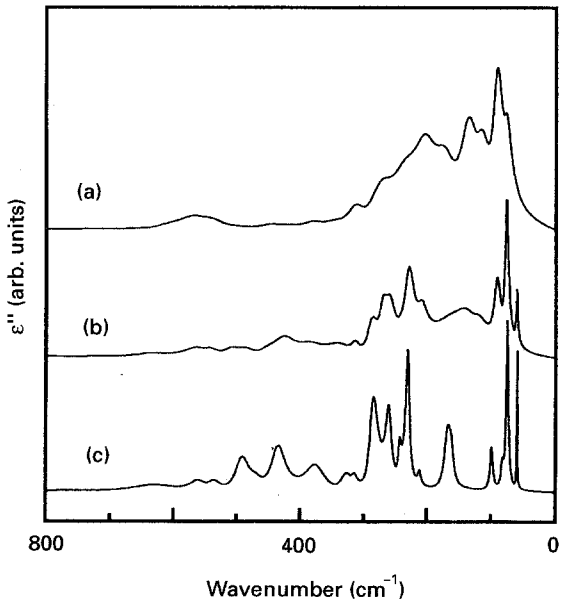

Figure 9 Computed ε'' as a function of frequency for (a) $BaPr_2Ti_4O_{12}$, (b) $0.64BaTi_4O_9$–$0.36BaPr_2Ti_4O_{12}$, and (c) $BaTi_4O_9$ ceramics.

TABLE III Measured and calculated dielectric characteristics at 5 GHz

Material	Measured		Calculated	
	ε_r	Q (at 5 GHz)	ε_r	Q (at 5 GHz)
$BaTi_4O_9$	35	10200	37	9700
$0.64BaTi_4O_9$–$0.36BaPr_2Ti_4O_{12}$	57	1890	56	4200
$BaPr_2Ti_4O_{12}$	91	1000	90	2300

4. Conclusions

The microwave characteristics of the system $BaTi_4O_9$–$BaPr_2Ti_4O_{12}$ were investigated, including its microstructure and infrared reflection spectroscopy. The following results were obtained.

1. The system $BaTi_4O_9$–$BaPr_2Ti_4O_{12}$ is entirely composed of two phases, and it is suggested that the lattices of each phase are well matched obliquely at the interface in the sintered ceramics.
2. The mixing relation for Q values can be well applied to this system.
3. It would be possible to investigate the dielectric properties of ceramic materials composed of mixed phases by means of infrared reflection analysis.

Acknowledgements

We thank Mr K. Shoda and Mr A. Kunishige of Ube Scientific Analysis Laboratory, Inc., for their assistance in the experiment and also thank Professor M. Hano, Professor Y. Cho, and Dr H. Kubo for their helpful discussions.

References

1. S. KAWASHIMA, M. NISHIDA, I. UEDA and H. OUCHI, *J. Amer. Ceram. Soc.* **66** (1983) 421.
2. H. M. O'BRYAN, Jr, J. THOMSON, Jr and J. K. PLOURDE, *ibid.* **57** (1974) 450.
3. S. KAWASHIMA, M. NISHIDA. I. UEDA and H. OUCHI, Paper presented at the 87th Annual Meeting, American Ceramic Society, Cincinnati, OH, 6 May 1985 (Electronics Division Paper No. 15-E85).
4. A. E. PALADINO, *J. Amer. Ceram. Soc.* **54** (1971) 1689.
5. K. FUKUDA, R. KITOH and I. AWAI, *Jpn J. Appl. Phys.* **32** (1993) 4584.
6. S. NISHIGAKI, H. KATO, S. YANO and R. KAMIMURA, *Amer. Ceram. Soc. Bull.* **66** (1987) 1405.
7. F. GERVAIS and B. PIRIOU, *Phys. Rev.* **B10** (1974) 2038.
8. J. L. SERVOIN, F. GERVAIS, A. M. QUITTET and Y. LUSPIN, *ibid.* **B21** (1980) 2038.
9. R. M. LYDDANE, R. G. SACHS and E. TELLER, *ibid.* **59** (1951) 673.
10. T. KUROSAWA, *J. Phys. Soc. Jpn* **16** (1961) 1298.
11. K. WAKINO, M. MURATA and H. TAMURA, *J. Amer. Ceram. Soc.* **69** (1986) 34.
12. T. NEGAS, R. S. ROTH, H. S. PARKER and D. MINOR, *J. Solid State Chem.* **9** (1974) 297.
13. D. KOLAR, S. GABERSCEK, B. VOLAVSEK, H. S. PARKER and R. S. ROTH, *ibid.* **38** (1981) 158.
14. JCPDS cards: 35-228 for $BaPr_2Ti_4O_{12}$, 34–70 for $BaTi_4O_9$.
15. A. M. GENS, M. B. VARFOLOMEEV, V. S. KOSTROMAROV and S. S. KOROVIN, *Russian J. Inorg. Chem.* **26** (1981) 482.

16. M. B. VARFOLOMEEV, A. S. MIRONOV, V. S. KOSTOMAROV, L. A. GOLUBTSOVA and T. A. ZOLOTOVA, *Russian J. Inorg. Chem.* **33** (1988) 607.
17. W. G. SPITZER, R. C. MILLER, D. A. KLEINMAN and L. E. HOWARTH, *Phys. Rev.* **126** (1962) 1710.
18. S. G. MHAISALKAR, D. W. READEY, S. A. AKBAR, P. K. DUTTA, M. J. SUMNAR, and R. ROKHLIN, *J. Solid State Chem.* **95** (1991) 275.
19. R. KUDESIA, A. E. MCHALE, R. A. CONDRATE, Sr and L. R. SNYDER, *J. Mater. Sci.* **28** (1993) 6569.
20. K. FUKUDA, I. FUJII, R. KITOH, Y. CHO and I. AWAI, *Jpn J. Appl. Phys.* **32** (1993) 1712.

Received 9 February
and accepted 6 July 1994